

DAMAGE LOCATION IN STEEL-CONCRETE COMPOSITE BEAMS USING ENERGY TRANSFER RATIO (ETR)

TOMASZ WRÓBLEWSKI, MAŁGORZATA JAROSIŃSKA

West Pomeranian University of Technology, Department of Theory of Structure, Szczecin, Poland

e-mail: wroblewski@zut.edu.pl, jarosinska@zut.edu.pl

STEFAN BERCZYŃSKI

West Pomeranian University of Technology, Institute of Manufacturing Engineering, Szczecin, Poland

e-mail: Stefan.Berczynski@zut.edu.pl

The paper suggests a method of how to locate damage in steel-concrete beams using the energy transfer ratio (ETR). The initial numerical analyses performed for a simple model with 12 degrees of freedom confirmed the effectiveness of using the method for locating changes taking place in a structure. Successive analyses were conducted for a composite beam whose numerical model was developed in convention of the rigid finite element method RFE. Damage was introduced into the model, which was later localized on the basis of changes in the ETR.

Key words: steel-concrete composite beams, damage localization, energy transfer ratio (ETR)

1. Introduction

The issue of using modal analysis for damage detection and location in civil engineering structures has been the subject of many studies conducted for years all over the world. Traditional modal parameters, such as frequencies, mode shapes and damping ratios are not sensitive enough to damage, particularly in early phases of damage processes. New indices are being sought that could both inform about structural changes and point out their locations. Early detection of damage makes it possible to take quick remedial measures, not allowing the structure to be withdrawn from operation.

The present paper is a continuation of the earlier work by Wróblewski *et al.* (2011), which demonstrates how the Energy Transfer Ratio – ETR changes as a result of damage in steel-concrete connections of composite beams. The obtained results confirmed that ETR is more sensitive to changes in steel-concrete connection than the frequency of natural vibration or the damping ratio. Consequently, ETR can be used for damage detection in composite beams and other constructions. However, it should be pointed out that the earlier mentioned modal parameters were determined for the whole system. The global character of the parameters means that it is possible to detect damage, but it is impossible to define its location. This paper presents a method of damage location using ETR determined locally. To this end, a system must be divided into fragments for whom ETR is successively determined. Analysis of ETR changes defined for particular parts makes it possible to locate the area of damage.

2. The state-of-the-art

As mentioned earlier, research of how to use modal parameters for damage location has been conducted all over the world for many years now. Alampalli *et al.* (1995) presented the results of tests conducted on a real bridge which had been withdrawn from use. The bridge consisted

of two single-span steel girders with an integral concrete deck. Damage was introduced into the bridge through cutting the girder in different areas. The scholars analyzed changes of traditional parameters in reaction to the introduced damage. MAC – Modal Assurance Criterion (Allemang and Brown, 1982) was used to analyze the form of vibration. MAC was determined on the basis of the relation

$$\text{MAC}(\varphi_u, \varphi_d) = \frac{|\varphi_u^T \varphi_d^*|^2}{(\varphi_u^T \varphi_u^*)(\varphi_d^T \varphi_d^*)} \quad (2.1)$$

where φ_u and φ_d are the mode shapes in the undamaged and damaged state, * is the complex conjugate. MAC takes scalar values from 0 to 1 depending on the degree of correlation between the two modes. The research conducted by Alampalli *et al.* (1995) demonstrated that MAC parameter is not sensitive enough to sustained damage. It was experimentally confirmed that the frequency of vibrations was more sensitive to damage and it should be used for the purposes of damage detection.

Another example of how modal analysis is used to identify damage in composite constructions is provided by research conducted by a team of scientists from Italy (Dilena and Morassi, 2003, 2004; Morassi and Rochetto, 2003). The scientists presented results of the research they conducted on composite beams with damaged steel-concrete connection. Two pairs of beams were analyzed. The pairs differed with degree of connection; whereas one pair was partly connected, the other one was fully connected. The authors concluded that frequencies of axial vibrations of the beam were not very sensitive to damage of the connection. However, frequencies of flexural vibrations proved to be quite sensitive to damage. The differences amounted to 38%.

Liang and Lee (1991) defined a new modal parameter – Energy Transfer Ratio (ETR), which determines the amount of energy transferred between vibration modes. The authors maintained that the parameter was much more sensitive to damage than the traditional modal parameters (Huang *et al.*, 1996). Moreover, the parameter could be determined both globally (for the whole system) and locally (for successive parts of the system) (Lee and Liang, 1999), owing to which it could be a good identifier of damage location.

Kong *et al.* (1996) conducted research on a model of a composite bridge. The model made at a scale of 1:6 consisted of three steel girders which supported a concrete slab. The authors analyzed changes of modal parameters including natural frequency, damping ratio and ETR, which happened as a result of one kind of damage – removal of the support in one of the girders. The scientists confirmed that ETR is the most sensitive parameter to changes introduced in the construction, and when determined locally, it can successfully locate damage.

Lee and Liang (1999), while continuing studies begun by their predecessors, carried out research on the same model of the same bridge. Two kinds of damage were introduced that time into the model: (i) removal of the support in one of the girders, (ii) crack in the stretched part of the girder in one of the spans. The results confirmed that ETR was more sensitive to damage than the natural frequency or damping ratio. The area for which ETR displayed the largest changes overlapped with that where the damage occurred.

In-depth analyses of damage detection were presented by Wang and Zong (2002, 2003). Their research focused on analyzing the basic modal parameters and ETR, and was conducted on a model of a composite bridge made at a scale of 1:6. The model consisted of a concrete slab supported on four steel girders. The scientists analyzed two kinds of artificial damage: (i) loss of the support; (ii) out-of-plane buckling and cracking of the steel girder. The study demonstrated that out of the investigated parameters, ETR displayed the largest changes due to damage. Also, when determined locally, it turned out to be a good indicator of the areas where damage occurred.

As mentioned, an earlier research into how to apply modal analysis for damage detection has been conducted for more than ten years now. The quoted studies indicate that traditionally

defined modal parameters are not sensitive enough to structural changes and therefore new parameters are being sought. ETR is an example of such a new parameter. Studies found in the literature, where ETR analysis was used, were performed on models of composite bridges for two kinds of damage: (i) loss of a support, (ii) cracking of a steel girder.

The aim of the present study is to examine ETR for a simpler object, such as a steel-concrete composite beam with a constant section and with local damage of connection and the concrete slab. Contrary to the previous article (Wróblewski *et al.*, 2011) ETR will be determined locally for successive elements of the beam. Owing to this, it will be possible to locate the area of damage. Before conducting final analyses of the composite beam with damage, preliminary simulations will be carried out for a simpler system with 12 degrees of freedom. The obtained results are presented in the next section.

3. The twelve degree-of-freedom model

3.1. The model

Initial numerical analyses aiming at showing changes in the locally determined ETR were conducted for a system with 12 degrees of freedom. The system consisted of 12 elements, each with a mass of 6 kg. The masses were connected one with another by means of spring elements with a constant stiffness of 36 000 N/m and with damping elements from a range of 6-18 N s/m (according to Fig. 1). The system was fixed at both ends.

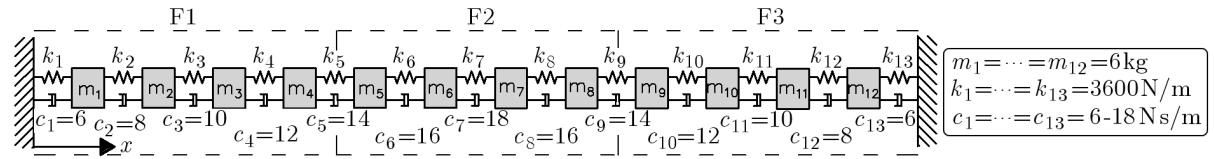


Fig. 1. 12-DOF model with division into parts

To determine local values of ETR, the system was broken down into three fragments: F1, F2, F3 (Fig. 1). Each of the fragments encompassed 4 masses. At first, ETR for F1, F2 and F3 in an undamaged state was determined. Then, analyses of damaged spring elements were performed. The damage was each time defined as lowering the stiffness of a given spring by 10%. Four cases were investigated: (i) D1 – damage defined as lowering the stiffness of spring k_2 , (ii) D2 – damage of spring k_3 ; (iii) D3 – damage of springs k_2 and k_3 ; (iv) D4 – damage of spring k_6 .

3.2. Determination of local ETR

The equation of free vibration motion for a system with n degrees of freedom takes the following form

$$\mathbf{M}\mathbf{X}'' + \mathbf{C}\mathbf{X}' + \mathbf{K}\mathbf{X} = \mathbf{0} \quad (3.1)$$

where: \mathbf{M} , \mathbf{C} , \mathbf{K} are the mass, damping and stiffness matrices ($n \times n$), \mathbf{X}'' , \mathbf{X}' , \mathbf{X} – acceleration, velocity and displacement vectors ($n \times 1$).

The above equation can also be given as

$$\mathbf{Y}'' + \overline{\mathbf{C}}\mathbf{Y}' + \overline{\mathbf{K}}\mathbf{Y} = \mathbf{0} \quad (3.2)$$

where: $\overline{\mathbf{C}}$, $\overline{\mathbf{K}}$ are generalized damping and stiffness matrices and

$$\overline{\mathbf{C}} = \mathbf{M}^{-\frac{1}{2}}\mathbf{C}\mathbf{M}^{-\frac{1}{2}} \quad \overline{\mathbf{K}} = \mathbf{M}^{-\frac{1}{2}}\mathbf{K}\mathbf{M}^{-\frac{1}{2}} \quad \mathbf{Y} = \mathbf{M}^{\frac{1}{2}}\mathbf{X} \quad (3.3)$$

For the system described by equation (3.2) there is a set of modal parameters such as natural frequencies ω_i , damping ratios ξ_i and mode shapes \mathbf{P}_i , where $i = 1, \dots, n$.

The matrix \mathbf{Q}_i is the eigenvector matrix of the generalized stiffness matrix $\overline{\mathbf{K}}$ (that is $\mathbf{Q}_i^T \mathbf{Q}_i = 1$). The relationship

$$\mathbf{Q}_i = \mathbf{P}_i \quad (3.4)$$

is true only for proportionally damped systems. For non-proportionally damped systems, for which $\mathbf{Q}_i \neq \mathbf{P}_i$ there is a relationship (Liang and Lee, 1991)

$$\frac{1}{2\omega_i} \left[\frac{\mathbf{Q}_i^T \overline{\mathbf{C}} \mathbf{P}_i}{\mathbf{Q}_i^T \mathbf{P}_i} \right] = \xi_i + j\zeta_i \quad (3.5)$$

where $j = \sqrt{-1}$. The real part of the right side of the equation is the conventionally defined damping ratio ξ_i . The imaginary part, which is to be found only for a system non-proportionally damped is called the energy transfer ratio ζ_i – ETR.

Using Equation (3.5), it is possible to determine ETR globally – for the whole system. In this case, it is necessary to use the matrix $\overline{\mathbf{C}}$ and all the vectors \mathbf{Q}_i and \mathbf{P}_i corresponding to several natural vibration ω_i . Formula (3.5) can be used to determine ETR locally – for successive fragments of the system. To determine ETR for a selected fragment of the system, it is necessary to use an appropriate part of the matrix $\overline{\mathbf{C}}$ and appropriate components of the vectors \mathbf{Q}_i and \mathbf{P}_i .

We present below a method of determining ETR for the analyzed model with 12 DOFs for fragment F2 and the first frequency of vibration. To this end, firstly, the imaginary left hand side of Equation (3.5) must be determined

$$\text{Im} \left(\frac{1}{2\omega_1} \left[\frac{\mathbf{Q}_{1,(5:8)}^T \overline{\mathbf{C}}_{(5:8),(5:8)} \mathbf{P}_{1,(5:8)}}{\mathbf{Q}_{1,(5:8)}^T \mathbf{P}_{1,(5:8)}} \right] \right) = \zeta_{1,(5:8)} \quad (3.6)$$

where

ω_1 – angular frequency of the first mode of vibration,

$\mathbf{Q}_{1,(5:8)}$ and $\mathbf{P}_{1,(5:8)}$ – fragments of vector \mathbf{Q} and vector \mathbf{P} (lines 5:8, gray), respectively, which corresponds to the first mode of vibration

$$\mathbf{Q} = \begin{bmatrix} Q_{1,1} & Q_{2,1} & \cdots & Q_{12,1} \\ Q_{1,2} & Q_{2,2} & \cdots & Q_{12,2} \\ Q_{1,3} & Q_{2,3} & \cdots & Q_{12,3} \\ Q_{1,4} & Q_{2,4} & \cdots & Q_{12,4} \\ \mathbf{Q}_{1,(5:8)} & \mathbf{Q}_{2,(5:8)} & \cdots & \mathbf{Q}_{12,(5:8)} \\ Q_{1,6} & Q_{2,6} & \cdots & Q_{12,6} \\ Q_{1,7} & Q_{2,7} & \cdots & Q_{12,7} \\ Q_{1,8} & Q_{2,8} & \cdots & Q_{12,8} \\ Q_{1,9} & Q_{2,9} & \cdots & Q_{12,9} \\ Q_{1,10} & Q_{2,10} & \cdots & Q_{12,10} \\ Q_{1,11} & Q_{2,11} & \cdots & Q_{12,11} \\ Q_{1,12} & Q_{2,12} & \cdots & Q_{12,12} \end{bmatrix} \quad \mathbf{P} = \begin{bmatrix} P_{1,1} & P_{2,1} & \cdots & P_{12,1} \\ P_{1,2} & P_{2,2} & \cdots & P_{12,2} \\ P_{1,3} & P_{2,3} & \cdots & P_{12,3} \\ P_{1,4} & P_{2,4} & \cdots & P_{12,4} \\ \mathbf{P}_{1,(5:8)} & \mathbf{P}_{2,(5:8)} & \cdots & \mathbf{P}_{12,(5:8)} \\ P_{1,6} & P_{2,6} & \cdots & P_{12,6} \\ P_{1,7} & P_{2,7} & \cdots & P_{12,7} \\ P_{1,8} & P_{2,8} & \cdots & P_{12,8} \\ P_{1,9} & P_{2,9} & \cdots & P_{12,9} \\ P_{1,10} & P_{2,10} & \cdots & P_{12,10} \\ P_{1,11} & P_{2,11} & \cdots & P_{12,11} \\ P_{1,12} & P_{2,12} & \cdots & P_{12,12} \end{bmatrix}$$

$\overline{C}_{(5:8),(5:8)}$ – a fragment of the matrix \overline{C} (lines 5:8, columns 5:8; gray)

$$\overline{C}_{(5:8),(5:8)} = \begin{bmatrix} c_{1,1} & \cdots & c_{5,1} & c_{6,1} & c_{7,1} & c_{8,1} & \cdots & c_{12,1} \\ \cdots & \cdots & \cdots & \cdots & \cdots & \cdots & \cdots & \cdots \\ c_{1,5} & \cdots & c_{5,5} & c_{6,5} & c_{7,5} & c_{8,5} & \cdots & c_{12,5} \\ c_{1,6} & \cdots & c_{5,6} & c_{6,6} & c_{7,6} & c_{8,6} & \cdots & c_{12,6} \\ c_{1,7} & \cdots & c_{5,7} & c_{6,7} & c_{7,7} & c_{8,7} & \cdots & c_{12,7} \\ c_{1,8} & \cdots & c_{5,8} & c_{6,8} & c_{7,8} & c_{8,8} & \cdots & c_{12,8} \\ \cdots & \cdots & \cdots & \cdots & \cdots & \cdots & \cdots & \cdots \\ c_{1,12} & \cdots & c_{5,12} & c_{6,12} & c_{7,12} & c_{8,12} & \cdots & c_{12,12} \end{bmatrix}$$

$\zeta_i = \zeta_{1,(5:8)}$ – ETR determined locally for fragment F2 which corresponds to the first mode of vibration.

3.3. Results of the conducted analysis

On the basis of expression (3.6), ETR was determined for a state without any damage and for a state with damage in fragments F1, F2 and F3. The first three forms of natural vibration were analyzed. The sensitivity of locally determined ETR to structural changes was defined using the indicator Δ_i [%] calculated using the following relation

$$\Delta_i = \left| \frac{\zeta_{i,d} - \zeta_{i,u}}{\zeta_{i,u}} \right| \quad (3.7)$$

where $\zeta_{i,d}$ and $\zeta_{i,u}$ stand for ETR in the damaged and undamaged state, respectively.

Figure 2 presents the model with 12 DOFs in the undeformed and deformed state corresponding to the fundamental natural frequency. The normalized mode shape vectors are presented on curves in Fig. 3a. The displacements of individual masses in the x -direction were put on the vertical axis of ordinates. The curves show mode shapes in the undamaged and damaged state. Both mode shapes were broken down into three fragments F1, F2, F3, and for each fragment the ETR value was determined as shown in Fig. 3b. Figure 3c shows the percentage change in the ETR after the damage was introduced.

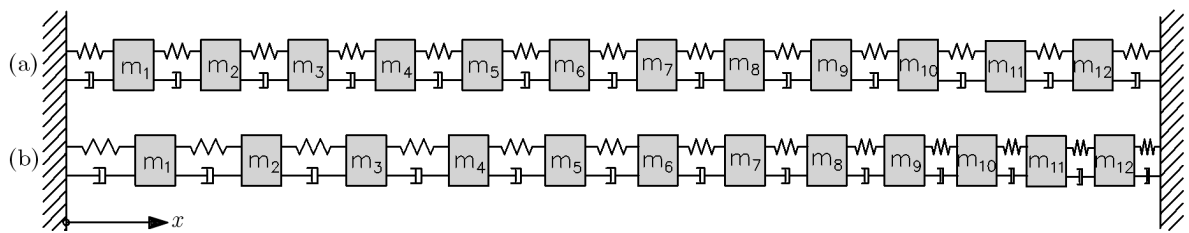


Fig. 2. 12-DOF model: (a) undeformed; (b) first mode shape in the undamaged state

The results of analysis conducted for successive forms of damage (D1, D2, D3, D4) are presented in a graphical form in Fig. 4.

As can be seen from the above presented curves, the most significant changes of the local ETR occur in the areas where damage also occurred. For D1 and D2, damage occurred in the same fragment F1, if for different springs: D1 – for k_2 and D2 – for k_3 . According to Figs. 4a,b, the maximum changes of ETR, which defined the damaged areas, were D1 – 11% and D2 – 7%, respectively. The next damage D3 was modeled to verify that with the

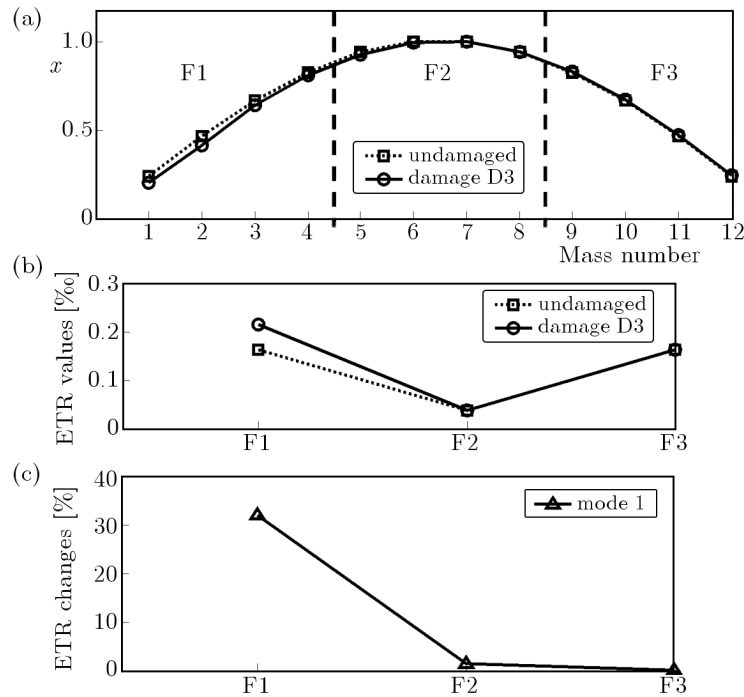


Fig. 3. Analysis of the first mode shape: (a) mode shapes before and after damage D3, (b) ETR values for fragments F1-F3, (c) ETR changes

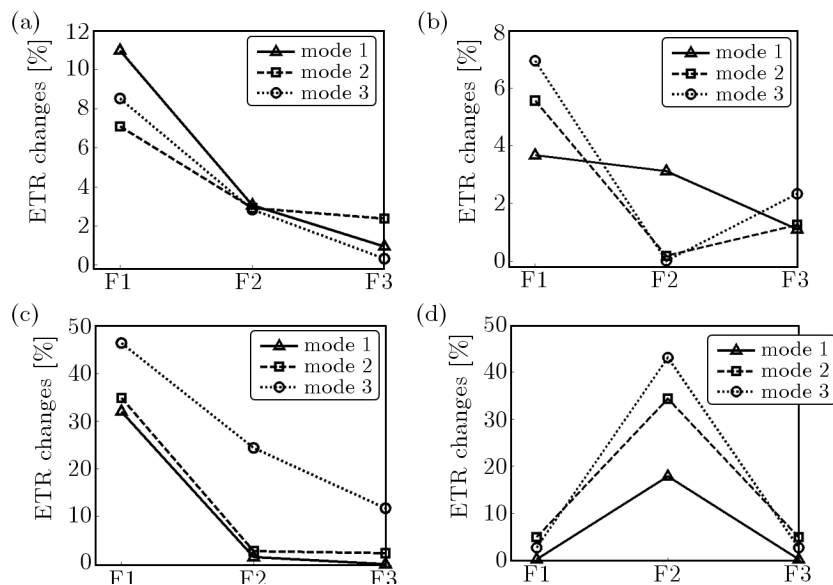


Fig. 4. ETR changes for: (a) damage D1, (b) damage D2, (c) damage D3, (d) damage D4

increase of the damage area there also grows the value of index Δ_i . Damage D3 in its scope covers the damage of two springs: k_2 and k_3 (which were also analyzed separately as damages D1 and D2). The maximum change of ETR in this case was 46%. This means that when the damaged area increases, the coefficient Δ_i increases as well. High sensitivity damage detection of ETR for the above mentioned simple twelve degree-of-freedom model confirms the usefulness of analyzing local ETR in more complex systems, such as steel-concrete composite beams.

4. Composite beam

4.1. The subject of the study

The beam cross-section is presented in Fig. 5. The beam measured 3200 mm in overall length. The beam consisted of a rolled steel I-bar IPE 160 made of S235JRG2 steel and a reinforced concrete slab 60×600 mm in the section size made of C25/30 concrete.

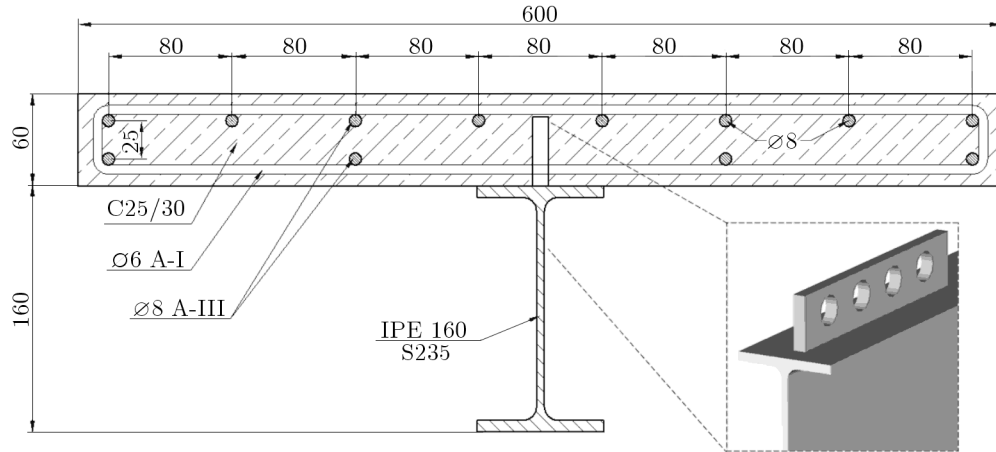


Fig. 5. The cross-section of the composite beam

The beam had a fixed connection which was made of connecting elements manufactured from a steel flat bar, 10 mm in thickness, made of S235JRG2 steel. The distribution of the connecting elements is shown in Fig. 6.

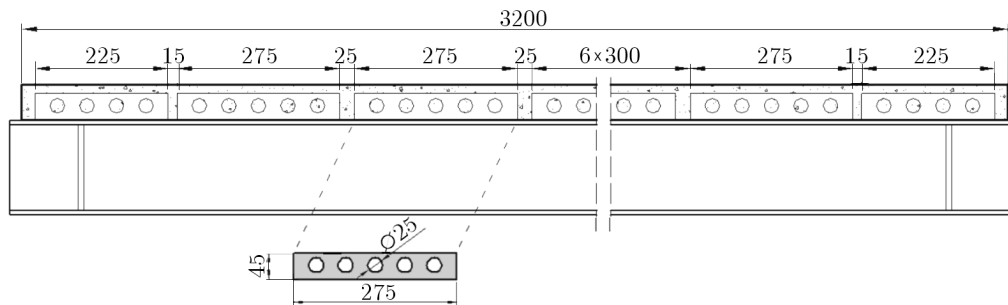


Fig. 6. The distribution of connecting elements

The tests on the beam, whose aim was to determine basic dynamic characteristics, were conducted on a free beam. This kind of beam was achieved by suspending the tested beam on two steel frames by means of four steel cables. Table 1 contains vibration frequencies and the values of their corresponding modal damping ratios for the first five flexural vibration modes of the beam.

Table 1. Experimental natural vibration frequencies and their corresponding values of modal damping ratio

i	1_{flex}	2_{flex}	3_{flex}	4_{flex}	5_{flex}
f_i [Hz]	77.75	186.65	304.72	417.57	531.13
ξ_i [%]	0.11	0.27	0.33	0.42	0.42

4.2. The model of the beam

The numerical model of the beam has been created in convention of the rigid finite element method – RFE model (Kruszewski *et al.*, 1975; Wittbrodt *et al.*, 2006). The central idea of the method is the division of a real system into rigid bodies which are called rigid finite elements (RFE), which are then in turn connected by means of spring-damping elements (SDE).

The analyzed beam was segmented into $n = 32$ sections, 100 mm in length each, which eventually produced a model consisting of 66 rigid finite elements RFEs connected by means of 97 spring-damping elements SDEs (Fig. 7).

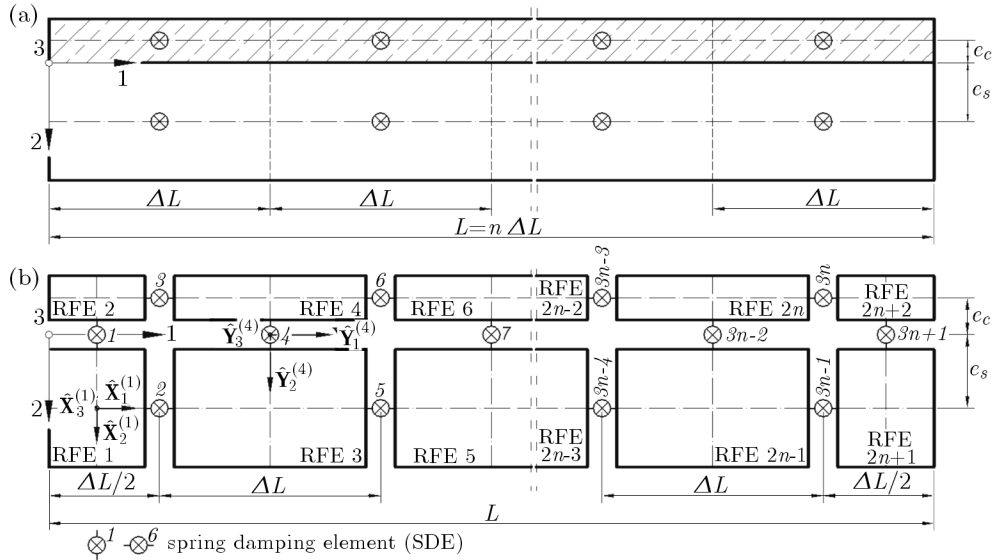


Fig. 7. RFE model: (a) segmentation of the beam into sections (primary division); (b) RFE system (secondary division)

The basic parameters necessary to define the model: (i) for the reinforced concrete slab – t_c , A_c , I_c , ρ_c , e_c ; (ii) for the rolled steel I-bar – A_s , I_s , ρ_s , e_s , E_s , were determined on the basis of inventory and literature data. The three remaining parameters necessary to define the model, i.e. the substitute modulus of elasticity (Young’s modulus) of the reinforced concrete slab E_c and the stiffness of connection along both directions K_h , K_v were identified on the basis of parametric identification. The identification criteria included the best fit of natural vibration frequency obtained in tests in numerical analyses. Table 2 contains the values of the identified parameters.

Table 2. Parameters of the model determined on the basis of parametric identification

K_h [N/m]	2.012E+09
K_v [N/m]	2.745E+08
E_c [N/m ²]	3.392E+10

The loss factor Q^{-1} was used to define the damping parameters of the structure. The relations between the elements of the stiffness matrix k_{ij} and damping matrix c_{ij} were determined on the basis of the following equation

$$c_{ij} = \frac{Q^{-1}}{\omega} k_{ij} \quad (4.1)$$

where ω is the vibration frequency. Values of the loss factor for steel, concrete and connections were estimated by fitting frequency response characteristics obtained from the RFE model to

characteristics obtained in the tests. Such values of the loss factor were sought for which the amplitudes of characteristics for selected resonance frequencies obtained experimentally and numerically overlapped. The loss factors determined in the analysis were: (i) for steel – 0.0003; (ii) for concrete – 0.0222; (iii) for connections – 0.0058.

More detailed information about the investigated beam and its model is available in the earlier study – Wróblewski *et al.* (2011).

4.3. Numerical simulation of damage

The numerical simulation of damage planned for the composite beam model was aimed at defining the damaged area. A locally determined ETR was the parameter which was supposed to locate the damaged areas. Additionally, changes of global modal parameters, such as frequency of natural vibration, damping ratio and global ETR were analyzed as well. The degree of changes in mode shapes was also assessed using the MAC parameter according to (2.1).

In order to determine local values of ETR, the analyzed composite beam was divided into three fragments – F1, F2 and F3. Three kinds of damage were introduced into fragments F1 and F2: D1 – damage of connection, D2 – damage of concrete slab, D3 – damage of both the connection and the slab. The lengths between one end of the beam and the damaged area were: (i) 350 mm for fragment F1, (ii) 1550 mm for fragment F2 (Fig. 8).

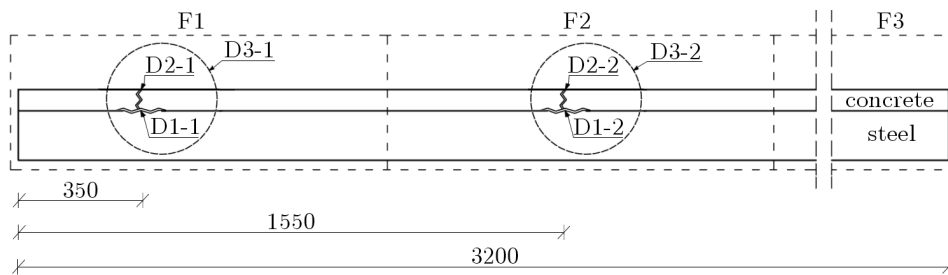


Fig. 8. The distribution of damage in the composite beam

Every fragment of the beam, i.e. F1, F2 and F3 consisted in the model of 22 rigid finite elements, 11 for the steel section and 11 for the concrete slab. The analysis began from determining ETR values for each fragment in the undamaged state. The values are presented in Table 3.

Table 3. ETR values for selected fragments in an undamaged state

$\zeta_{i,u}$ [%]	i	F1	F2	F3
	1_{flex}	0.179	0.294	0.179
	2_{flex}	0.075	0.043	0.075
	3_{flex}	0.036	0.044	0.036

The next step of the analysis was to simulate damage of the beam. The damage was modeled through lowering the stiffness coefficient of selected spring-damping elements which modeled the connection or the slab. The degree of range of damage was defined in the following way: (i) to simulate damage of connection D1, the stiffness of two adjacent SDEs was reduced by 50%; (ii) to simulate damage of concrete slab D2, the stiffness of one SDE was reduced by 25%; (iii) damage of the connection and concrete slab D3 was a sum of D1 and D2 combined damage. Table 4 presents a list of the analyzed damage cases as well as numeration of SDEs which were damaged in particular cases. The numeration of SDEs is consistent with Fig. 7. For D1-1 and D2-1 cases, Fig. 9 shows in a graphical way the SDEs which were reduced.

Table 4. A description of the analyzed damage

Type of damage		Location of damage		
		Damaged fragment	Damaged SDEs*	
			Connection (1, 4, 7, ..., 3n + 1)	Concrete slab (3, 6, 9, ..., 3n)
Connection	D1-1	F1	10, 13	–
	D1-2	F2	46, 49	–
Concrete slab	D2-1	F1	–	12
	D2-2	F2	–	48
Connection and concrete slab	D3-1	F1	10, 13	12
	D3-2	F2	46, 49	48

* The numeration of SDEs is consistent with the diagram presented in Fig. 7

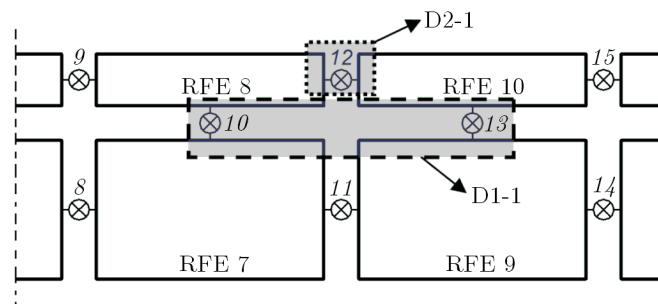


Fig. 9. Damage D1-1, D2-1

The assessment of the degree of change of the analyzed modal parameters was conducted for the first three forms of flexural vibrations. All the changes of parameters given globally are presented in Tables 5-8. The changes of ETR along the length of the beam are presented in a graphical form in Fig. 10.

Table 5. Changes in the frequencies of natural vibrations f_i

i	$f_{i,num}$ [Hz]	Damage					
		D1-1 Δ [%]	D1-2 Δ [%]	D2-1 Δ [%]	D2-2 Δ [%]	D3-1 Δ [%]	D3-2 Δ [%]
1	77.75	-0.08	-0.03	-0.01	-0.28	-0.09	-0.32
2	187.08	-0.19	-0.47	-0.02	-0.01	-0.22	-0.48
3	307.10	-0.25	-0.63	-0.07	-0.21	-0.33	-0.89

Table 6. Changes in the damping ratio ξ_i

i	$\xi_{i,num}$ [%]	Damage					
		D1-1 Δ [%]	D1-2 Δ [%]	D2-1 Δ [%]	D2-2 Δ [%]	D3-1 Δ [%]	D3-2 Δ [%]
1	0.26	0.33	0.17	0.09	3.51	0.41	3.82
2	0.28	0.69	1.51	0.32	0.09	0.99	1.61
3	0.33	0.72	3.18	0.58	1.23	1.37	5.14

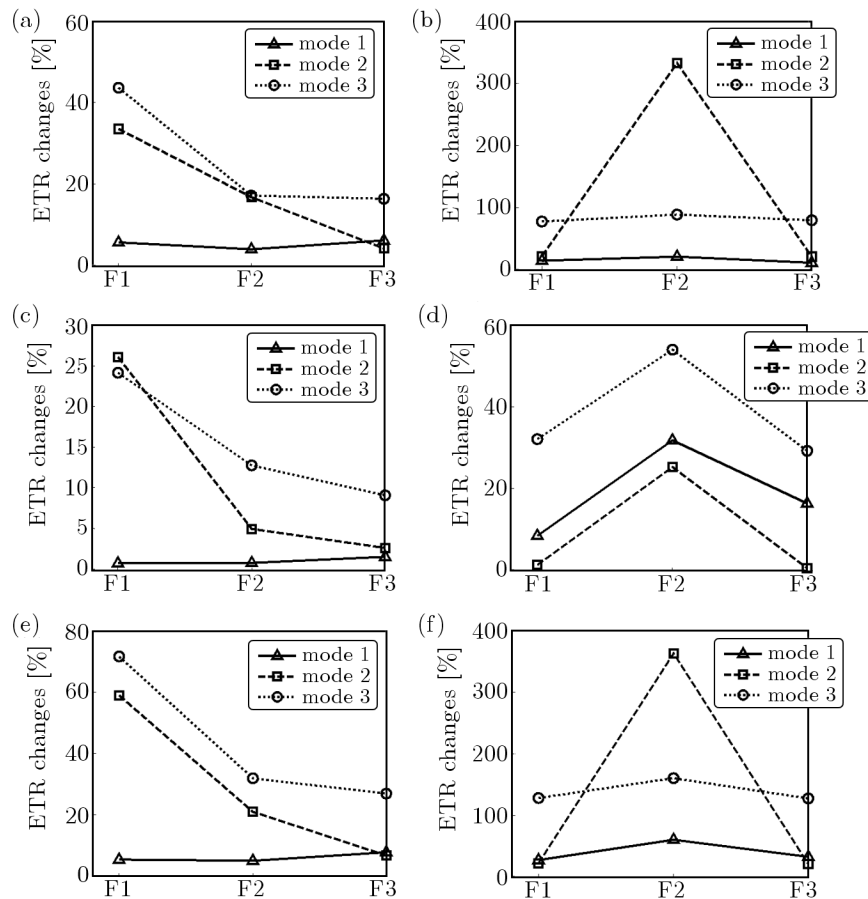
As the above tables show, out of the global modal parameters, ETR is the most sensitive to damage. The most marked changes of ETR were found for damage D3-2 and reached 14.02%. The corresponding change of the damping ratio was 5.14%, vibration frequency 0.89%, 1-MAC – 0.15%.

Table 7. Changes of ETR ζ_i

i	$\zeta_{i,num} \cdot 10^{-2}$ [%o]	Damage					
		D1-1 Δ [%]	D1-2 Δ [%]	D2-1 Δ [%]	D2-2 Δ [%]	D3-1 Δ [%]	D3-2 Δ [%]
1	2.55	-0.10	0.05	0.27	10.26	0.16	10.63
2	1.92	-0.35	-1.59	1.39	0.34	0.98	-1.23
3	1.39	-0.80	3.85	3.80	6.27	3.35	14.02

Table 8. (1-MAC)

i	Damage					
	D1-1 Δ [%]	D1-2 Δ [%]	D2-1 Δ [%]	D2-2 Δ [%]	D3-1 Δ [%]	D3-2 Δ [%]
1	0.00	0.00	0.00	0.00	0.00	0.00
2	0.01	0.01	0.00	0.00	0.01	0.01
3	0.02	0.06	0.01	0.02	0.04	0.15


Fig. 10. ETR changes: (a) damage D1-1, (b) damage D1-2, (c) damage D2-1, (d) damage D2-2, (e) damage D3-1, (f) damage D3-2

While analyzing the course of ETR changes along the length of the beam, changes in locally determined ETR in the damaged area are clearly seen. The biggest changes of ETR occurred for 2 vibration frequencies for damage D3-2 and amounted to over 350%. ETR turned out to be the least sensitive for the first vibration frequency. As expected, when the degree of damage increases, the absolute values of the coefficient Δ_i also increase.

5. Summary

The present paper, which is a continuation of the earlier work by Wróblewski *et al.* (2011), presents a method of damage location in steel-concrete composite beams using locally determined ETR. The initial analyses conducted for a model with 12 degrees-of-freedom produced satisfactory results as ETR significantly changes its values close to the area where a change in the stiffness occurred. Successive analyses performed for the steel-concrete composite beam confirmed high sensitivity of locally determined ETR to damage. It should also be pointed out that out of all the analyzed parameters, it is the ETR that displays the highest sensitivity to damage. This confirms findings obtained earlier by Wróblewski *et al.* (2011). Further research is shortly planned into numerical analysis of a larger number of vibration frequencies with a denser division of the beam. The division of the beam into a larger number of fragments will, most probably, mean that in the future analyses it will be necessary to take into consideration curvature changes in the mode shapes. An important aspect of the planned analyses will be confirmation of results obtained in empirical tests.

The project has been financed by the National Science Centre.

References

1. ALAMPALLI S., FU G., DILLON E.W., 1995, On the use of measured vibration for detecting bridge damage, *Proceedings Fourth International Bridge Engineering Conference*, 125-137
2. ALLEMANG R.J., BROWN D.L., 1982, Correlation coefficient for modal vector analysis, *Proceedings of the 1st IMAC*, Orlando, Florida, 110-116
3. DILENA M., MORASSI A., 2003, A damage analysis of steel-concrete composite beams via dynamic methods: Part II. Analytical models and damage detection, *Journal of Vibration and Control*, **9**, 5, 529-565
4. DILENA M., MORASSI A., 2004, Experimental modal analysis of steel concrete composite beams with partially damaged connection, *Journal of Vibration and Control*, **10**, 897-913
5. HUANG T.-J., LIANG Z., LEE G.C., 1996, Structural damage detection using energy transfer ratios (ETR), *Proceedings 14th International Modal Analysis Conference*, 126-132
6. KONG F., LIANG Z., LEE G.C., 1996, Bridge damage identification through ambient vibration signature, *Proceedings 14th International Modal Analysis Conference*, 717-724
7. KRUSZEWSKI J., GAWROŃSKI W., WITTBRODT E., NAJBAR F., GRABOWSKI S., 1975, *Metoda sztywnych elementów skończonych*, Arkady, Warszawa
8. MORASSI A., ROCCHETTO L., 2003, A damage analysis of steel-concrete composite beams via dynamic methods: Part I. Experimental results, *Journal of Vibration and Control*, **9**, 5, 507-527
9. LEE G.C., LIANG Z., 1998, On cross effects of seismic responses of structures, *Engineering Structures*, **20**, 4, 503-509
10. LEE G.C., LIANG Z., 1999, Development of a bridge monitoring system, *Proceedings of the 2nd International Workshop on Structural Health Monitoring*, Stanford University, Stanford, CA, 349-358
11. LIANG Z., LEE G.C., 1991, Damping of structures, Part 1, National Center for Earthquake Engineering Research, Technical Report NCEER-91-0004, State University of New York at Buffalo, Buffalo, NY
12. LIANG Z., TONG M., LEE G.C., 1995, Modal energy measurement of a long steel bridge, *Proceedings 13th International Modal Analysis Conference*, 226-232

13. MORASSI A., ROCCHETTO L., 2003, A damage analysis of steel-concrete composite beams via dynamic methods: Part I. Experimental results, *Journal of Vibration and Control*, **9**, 5, 507-527
14. WANG T.L., ZONG Z., 2002, Improvement of evaluation method for existing highway bridges (Final report No. FL/DOT/RMC/6672-818), Florida Department of Transportation, FL 32399, USA
15. WANG T.L., ZONG Z.H., 2003, Structural damage identification by using energy transfer ratio, *IMAC-XXI: A Conference on Structural Dynamics*, Kissimmee, Florida
16. WITTBRODT E., ADAMIEC-WÓJCIK I., WOJCIECH S., 2006, *Dynamics of Flexible Multibody Systems. Rigid Finite Element Method*, Springer-Verlag, Berlin, Heidelberg, New York
17. WRÓBLEWSKI T., JAROSIŃSKA M., BERCZYŃSKI S., 2011, Application of ETR for diagnosis of damage in steel-concrete composite beams, *Journal of Theoretical and Applied Mechanics*, **49**, 1, 51-70

Lokalizacja uszkodzeń w stalowo-betonowych belkach zespolonych za pomocą współczynnika transferu energii (ETR)

Streszczenie

W artykule przedstawiono propozycję metody lokalizacji uszkodzeń w stalowo-betonowych belkach zespolonych za pomocą współczynnika transferu energii ETR. Wstępne analizy numeryczne wykonane dla prostego modelu o 12 stopniach swobody potwierdziły skuteczność metody w lokalizacji zmian zachodzących w konstrukcji. Kolejne analizy przeprowadzono dla belki zespolonej, której model numeryczny wykonano w konwencji metody sztywnych elementów skończonych SES. Do modelu wprowadzono uszkodzenia, które następnie lokalizowano na podstawie zmiany ETR.

Manuscript received September 19, 2011; accepted for print March 19, 2012